Available online at www.sciencedirect.com

SCIENCE DIRECT®

International Journal of Heat and Mass Transfer 48 (2005) 403–412

International Journal of HEAT and MASS TRANSFER

www.elsevier.com/locate/ijhmt

Surprising effects of combined vapour and liquid mass transfer resistances when condensing a mixture outside tube banks

Tord Karlsson *, Lennart Vamling

Heat and Power Technology, Department of Chemical Engineering and Environmental Science, Chalmers University of Technology, SE-412 79 Gothenburg, Sweden

Received 13 February 2004; received in revised form 17 May 2004
Available online 12 October 2004

Abstract

Detailed calculations are carried out for condensation of a binary zeotropic mixture outside a tube bank to investigate combined effects of mass transfer resistances in the liquid and vapour phases. The question is how a change in mass transfer resistance in the vapour phase can influence the heat flux. The surprising result is that a decrease in resistance in the vapour phase by reducing the tube pitch, and thus increasing the vapour velocity, reduces the heat flux between 20% and 50% for the conditions studied. This is due to a combination of mass transfer resistance, depletion of the heavy volatile component, and a reduction of the phase interface temperature.

Keywords: Condensation; Mixture; Tube bundle; Mass transfer resistance

1. Introduction

1.1. Background

Condensation of mixtures is important in various fields of engineering, one of which is in condensers for heat pumps. If the mixtures are zeotropic, also called non-azeotropic, effects of gliding temperature difference (GTD) and mass transfer resistances can become apparent. GTD means a decrease in dew point temperature under the course of condensation; this is due to a composition shift caused by the preferential condensation of the less volatile component. A higher condensation rate of the less volatile component leaves the vapour enriched by the more volatile component, thus causing a lower dew point temperature for the remaining vapour. The other effect that can arise when condensing a zeotropic mixture, mass transfer resistance, can occur in both phases. The preferential condensation of the less volatile component causes a depletion of the less volatile component close to the interface. This means that the less volatile component must be transported through a film enriched by the more volatile component. The necessity of being transported through the film is called mass transfer resistance. Furthermore, if the mixing in the liquid film is insufficient, the less volatile component can accumulate at the liquid interface, thus creating a mass transfer barrier. A change in liquid composition at the interface will have two consequences: It will change the concentration gradient in the gas film closest

---

[*] Corresponding author. Tel.: +46 31 772 85 35; fax: +46 31 821 928.

E-mail addresses: tord.karlsson@hpt.chalmers.se (T. Karlsson), lennart.vamling@hpt.chalmers.se (L. Vamling).

0017-9310/$ - see front matter © 2004 Elsevier Ltd. All rights reserved.
doi:10.1016/j.ijheatmasstransfer.2004.06.041

Nomenclature

A_o	tube outside area
c_p	heat capacity
c_t	total molar concentration
D	liquid diffusivity
Đ	Maxwell–Stefan diffusivity
d_t	tube outside diameter
g	gravitational acceleration
h_c	heat transfer coefficient to coolant
h_fg	specific enthalpy of vapourization
h_g	heat transfer coefficient from vapour
J	diffusive flux
M	mass
N	condensing flux
p	pressure
Pr	Prandtl number
q	heat flux
Q	heat flux
R	fouling resistance
Sc	Schmidt number
T	temperature
u	velocity
V	molar volume
x	molar fraction in liquid
y	molar fraction in vapour
z	distance

Greek symbols

β	mass transfer coefficient
δ	film thickness
ϕ	rate factor
Γ	liquid flow
η	dimensionless distance
λ	thermal conductivity
μ	dynamic viscosity
θ	angle around tube
ρ	density

Superscripts

0	at infinite dilution
$\bullet$	corrected for mass transfer

Subscripts

b	bulk
c	coolant
g	vapour
I	interface
i	inside
i	component number
j	component number
l	liquid, condensate
m	molar
o	outside
θ	tangential direction
r	radial direction
t	total
tot	total
w	wall

to the interface, thus affecting the mass transport from the vapour bulk to the interface, but more importantly it will also influence the interface temperature. The interface temperature regulates the rate of heat transfer away from the interface. The higher the temperature, the higher the heat flux.

1.2. Previous work

According to the review article by Cavallini et al. [1], not a lot of work has been carried out on condensation of zeotropic mixtures in tube bundles. Handbooks such as Heat Exchanger Design Handbook [2] and VDI Wärmeatlas [3] treats the subject and give advice on calculation methods. Books by Bird et al. [4], Collier and Thome [5] and Stephan [6] also go into the subject. Experimental work on condensation outside bundles has also been presented. Honda et al. [7,8] tested different tube geometries in a tube bundle, and found a considerably lower heat transfer coefficient for all geometries for a mixture than for pure R123 and R134a. They concluded that the difference was greater for lower mass velocities and lower temperature differences, and that the reason is the diffusive transport resistance in the vapour film closest to the gas–liquid interface. Belghazi et al. [9,10] recorded a decrease of 30–50% in heat transfer coefficient for the mixture R23/R134a with the same explanation. Jung et al. [11,12] measured heat transfer coefficients for the mixture R407C on one smooth, horizontal tube, and found up to 50% lower heat transfer coefficients than for R22. Gabrielii and Vamling [13] studied R22 and three mixtures in a full-scale condenser, and found an up to 70% decrease in heat transfer for the mixtures.

In the experimental work referred to above, the authors state that diffusive transport resistance in the vapour phase is the reason for the decrease in heat transfer, more as a statement than as a result. Sajjan et al. [14] and Karlsson and Vamling [15] studied the condensate flow theoretically and concluded that besides the diffusive resistance in the vapour film closest to the interface, mass transfer resistance in the condensate is also an important factor for the decrease in heat transfer coefficients for mixtures.

From this it is apparent that mass transfer resistance is an important factor for mixture condensation, and that it is a topic that needs to be better understood.

1.3. Aim with this work

In this paper the combined effects of mass transfer resistances in the vapour and liquid phases are investigated. Since no experimental equipment exists where this can be measured, this theoretical study is carried out to try to enlighten the readers on the phenomenon. In order to give the phenomenon a measure, it is investigated to what degree it is possible to improve the rate of heat and mass transfer by simple means such as changing the tube pitch, i.e. the horizontal distance between the tubes. A decrease in tube pitch leads to higher vapour velocity, and therefore also to lower mass transfer resistance in the gas phase. This should in its turn mean a higher rate of condensation and therefore a higher rate of heat transfer.

In order to make the investigations, detailed calculations are carried out for condensation of a binary mixture outside a vertical tube column of ten horizontal tubes. A zeotropic mixture of the two refrigerants R134a and R32 is used. The horizontal tube pitch is varied, i.e. the smallest cross section area available for flow, which influences the vapour velocity, and thus also the mass transfer resistance. For different conditions and different tub pitches the tube length is then adjusted to obtain total condensation. The change in required tube length, which is the same as required heat transfer area, can then be used as a measure of the influence of mass transfer resistance.

2. Theory

In order to determine the rate of condensation for a mixture outside horizontal tubes, both heat and mass transfer relations have to be solved. The calculations carried out for this paper use a high level of detail, solving mass transfer rigorously in both phases. Each tube is divided into smaller calculation cells, shown in Fig. 1(b), in which all equations for heat and mass transfer described below are solved. The starting point for the calculations is an overall heat balance for a calculation cell:

$$\mathrm{d}Q = \mathrm{d}q_\mathrm{g} + \mathrm{d}q_\mathrm{l} + N_\mathrm{tot} \cdot h_\mathrm{fg} \cdot M_\mathrm{m} \tag{1}$$

where $\mathrm{d}Q$ is total heat transferred from the vapour bulk to the coolant flowing in the tube, $\mathrm{d}q_\mathrm{l}$ is sensible heat from cooling the condensate formed on tubes above, $\mathrm{d}q_\mathrm{g}$ is sensible heat from cooling the vapour, and h_fg is the latent heat of the condensing vapour flux N_tot. Even under saturated conditions and without pressure drop, the terms $\mathrm{d}q_\mathrm{l}$ and $\mathrm{d}q_\mathrm{g}$ will be present due to the gliding temperature difference of a zeotropic mixture. In order to get the composition of N_tot, mass transfer relations have to be solved.

2.1. Mass transfer theory in the liquid phase

The basic assumption for mass transfer in the liquid phase is that diffusion is the only transport mechanism, which also implies that the condensate flow is laminar, as was discussed by Karlsson and Vamling [15]. We begin with calculations of the thickness as well as the tangential velocity profile in the condensate film from a given total liquid flow Γ, the original Nusselt equations, taken from Bird et al. [4]:

$$\delta_\mathrm{l} = \left[\frac{3 \cdot \Gamma \cdot \mu_\mathrm{l}}{\rho_\mathrm{l}^2 \cdot g \cdot \sin(\theta)}\right]^{1/3} \tag{2}$$

$$u_\theta = \frac{(\rho_\mathrm{l} - \rho_\mathrm{g}) \cdot g \cdot \sin(\theta)}{\mu_\mathrm{l}} \cdot \left(y \cdot \delta_\mathrm{l} - \frac{y^2}{2}\right), \quad 0 \leqslant y \leqslant \delta_\mathrm{l} \tag{3}$$

where δ_l is the condensate film thickness and θ is the angle around the tube, calculated from the top. A mass balance between the present calculation cell and the cell above will give a velocity component normal to the tube, towards the tube wall, u_r. This component is small

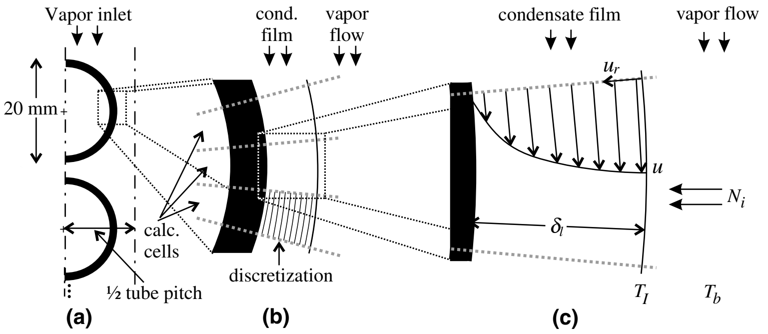

Fig. 1. Configuration for the tube bundle and for the calculation cells.

compared to the tangential velocity, but it is included when calculating mass transfer into the condensate.

When the velocity components are known, the diffusive transport of each component is calculated from Fick's first law of diffusive transport. For a binary mixture it can be expressed, according to Taylor and Krishna [16]:

$$J_{i,\mathrm{r}} = -c_\mathrm{t} D_{ij} \frac{\mathrm{d}x_i}{\mathrm{d}r}, \quad J_j = -J_i \tag{4}$$

$J_{i,\mathrm{r}}$ is the diffusive flux of component i in the radial direction, relative to the average velocity, here given by u_r, c_t is total concentration, $\mathrm{d}x_i/\mathrm{d}r$ is the concentration gradient of component i in the radial direction, and D_{ij} is the binary liquid diffusivity, here weighed together according to Vignes, as reported by Taylor and Krishna [16]:

$$D_{ij} = (D_{ij}^0)^{x_j}(D_{ji}^0)^{x_i} \tag{5}$$

x_i and x_j are molar fractions and D_{ij}^0 are liquid diffusion coefficients at infinite dilution, here calculated according to Siddiqi and Lucas [17]:

$$D_{ij}^0 = 9.89 \times 10^{-8} \mu_j^{-0.907} V_i^{-0.45} V_j^{0.265} T \tag{6}$$

where μ is viscosity [mPa s], V is molar volume [cm^3 mol^{-1}] and T is temperature [K]. From the equations above and the boundary conditions of zero diffusive flux through the wall and across the phase interface, the composition profile in the liquid film is solved, from which the surface composition will be known. This is needed for the mass transfer calculations in the vapour phase.

2.2. Mass transfer theory in the vapour phase

Assuming thermodynamic equilibrium between the phases at the interface, and with a known liquid interface composition, the interface composition in the vapour phase can be calculated from a relation of the form:

$$(y_\mathrm{I}, T_\mathrm{I}) = f(x_\mathrm{I}, p) \tag{7}$$

To solve the rate of mass transfer for each component, the Maxwell–Stefan equations are solved [16]:

$$\frac{\mathrm{d}y_1}{\mathrm{d}z} = \frac{(y_1 N_2 - y_2 N_1)}{c_\mathrm{t} Đ_{12}} \tag{8}$$

$$\frac{\mathrm{d}y_2}{\mathrm{d}z} = \frac{(y_2 N_1 - y_1 N_2)}{c_\mathrm{t} Đ_{21}} \tag{9}$$

where N_i are component molar fluxes, y are vapour phase concentrations, c_t total concentration, and $Đ_{ij}$ are binary Maxwell–Stefan diffusivities, estimated from Fuller et al. [18]. If a dimensionless distance coordinate is introduced, $\eta = z/\delta_\mathrm{g}$ where δ_g is the gas film thickness through which diffusion acts, then Eqs. (8) and (9) can be rewritten:

$$\frac{\mathrm{d}y_1}{\mathrm{d}\eta} = \frac{(y_1 N_2 - y_2 N_1)}{\beta_{\mathrm{g},12}} \tag{10}$$

$$\frac{\mathrm{d}y_2}{\mathrm{d}\eta} = \frac{(y_2 N_1 - y_1 N_2)}{\beta_{\mathrm{g},21}} \tag{11}$$

where $\beta_{\mathrm{g},ij}$ are binary mass transfer coefficients, defined as:

$$\beta_{\mathrm{g},ij} = c_\mathrm{t} \frac{Đ_{ij}}{\delta_\mathrm{g}} \tag{12}$$

For binary diffusion $Đ_{ij} = Đ_{ji}$, and thus $\beta_{\mathrm{g},ij}$ and $\beta_{\mathrm{g},ji}$ are of equal value. With the assumption that the transition between the vapour bulk molar fraction y_b and the interface molar fraction y_I takes place in the stagnant gas film of thickness δ_g and that the Chilton–Colburn analogy between heat and mass transfer [19] is valid, i.e.

$$j_\mathrm{H} = \frac{h_\mathrm{g}}{c_{p_\mathrm{g}}} Pr^{2/3} = j_\mathrm{D} = \beta_{\mathrm{g},ij} Sc^{2/3} \tag{13}$$

then the binary mass transfer coefficients, $\beta_{\mathrm{g},ij}$, can be calculated after inserting the expressions for Pr and Sc numbers:

$$\beta_{\mathrm{g},ij} = \frac{h_\mathrm{g}}{c_{p_\mathrm{g}}} \left(\frac{c_\mathrm{t} Đ_{ij} c_{p_\mathrm{g}}}{\lambda_\mathrm{g}} \right)^{2/3} \tag{14}$$

where h_g is the vapour phase heat transfer coefficient, described in the section below. This value of $\beta_{\mathrm{g},ij}$ is only valid for low net mass transfer rates, however, which is not the case with condensation. Therefore a correction is applied before the mass transfer coefficient is used in Eqs. (10) and (11). The correction has the form [4,16]:

$$\beta_{\mathrm{g},ij}^\bullet = \beta_{\mathrm{g},ij} \frac{\phi}{\mathrm{e}^\phi - 1} \tag{15}$$

where the dot on β means that it is corrected for mass transfer. The rate factor ϕ is defined as:

$$\phi = \frac{N_1 + N_2}{\beta_{\mathrm{g},ij}} \tag{16}$$

For the condensing system $\beta_{\mathrm{g},ij}^\bullet$ is used instead of $\beta_{\mathrm{g},ij}$ when solving the mass transfer equations.

2.3. Heat transfer theory

The composition of the condensing flux is determined from the mass transfer relations above, but in order to get the correct value for total condensing flux, the heat transfer relations must be solved. The starting point is Eq. (1), relating the total heat, dQ, that is conducted from the liquid–vapour interface through to the coolant inside the tube, to heat released by cooling the vapour, q_g, cooling the liquid, q_l, and latent heat from the condensing flux N_tot. Cooling of the liquid, q_l, is a consequence of the temperature glide for the mixture, and the temperature drop in the liquid can be calculated from the change in saturation temperature in the condensate. Cooling of the vapour can arise if the vapour is superheated at the inlet, but it will also be a consequence of the temperature glide, reducing the dew point temperature through the course of condensation. q_g can be calculated from:

$$q_g = h_g^{\bullet}(T_b - T_I) \tag{17}$$

where indices b and I stand for vapour bulk and interface respectively. The heat transfer coefficient in the vapour, h_g, is calculated according to Schmidt [20], and the dot means that the coefficient is corrected for mass transfer effects, here done according to Ackermann [21] and Colburn and Drew [22]. The effect of mass transfer on heat transfer may be underestimated with this method, but it is a commonly used method, and the magnitude of the correction will not have a great influence on the results, especially not on the trends. Furthermore, the calculations presented here are carried out locally on the tube, but tube average values are used for h_g in lack of more detailed heat transfer theory locally around individual tubes in tube banks.

The released thermal energy, dQ, in Eq. (1) must be transported from the vapour–liquid interface into the coolant flowing inside the tube, making a second relation necessary. It can be written:

$$\mathrm{d}Q = h_L(T_I - T_c)\mathrm{d}A_o \tag{18}$$

where indices I and c stand for interface and coolant respectively. h_L is the heat transfer coefficient from the condensate surface to the coolant, expressed by:

$$\frac{1}{h_L \mathrm{d}A_o} = \frac{1}{h_l \mathrm{d}A_o} + \frac{R_o}{\mathrm{d}A_o} + \frac{\delta_w}{\lambda_w \mathrm{d}A_w} + \frac{R_i}{\mathrm{d}A_i} + \frac{1}{h_c \mathrm{d}A_i} \tag{19}$$

where h_l is the coefficient for the condensate film, R is fouling, δ_w is tube wall thickness and h_c is the heat transfer coefficient inside the tube on the coolant side, here calculated from the Dittus–Boelter equation.

For local calculations in a laminar film, which is the case here, h_l can be calculated from pure conduction through the film:

$$h_l = \frac{\lambda_l}{\delta_l} \tag{20}$$

For the heat balance to be fulfilled, dQ calculated in Eq. (1) must equal that calculated in Eq. (18).

3. Calculation procedure

In order to solve the problem of binary mixture condensation on the outside of a tube column with horizontal tubes, an algorithm that solves for both heat and mass transfer simultaneously must be used. First, the tubes are divided into two along the vertical centre axis due to symmetry; see Fig. 1(a). The remaining half of each tube is then divided into 40 smaller calculation cells along the perimeter, as seen in Fig. 1(b). In each calculation cell the condensate film is further divided into smaller cells in the direction normal to the tube wall when calculating velocities and compositions in the liquid film, see discretization in Fig. 1(b). The solver works sequentially from the first calculation cell on the top tube, following the flow down to the last calculation cell on the bottom tube.

3.1. Algorithm

The algorithm is designed to solve heat and mass transfer simultaneously, and it is schematically shown in Fig. 2. The starting point is an assumption of condensing flux in a calculation cell, both in total flux and in composition. The next step is to calculate the film properties, the tangential velocities from Eq. (3) and the normal velocities from a mass balance. Then, since the condensing flux and composition is assumed, the differential Eq. (4) can be solved, and together with the velocities and the solution in the cell above, the composition profile in the condensate can be solved. From the solution the interface composition in the liquid is known, so Eq. (7) can be used to find the vapour interface composition. Then the heat transfer coefficient in the vapour phase is calculated, and from the heat and mass transfer analogy, Eq. (13), the mass transfer coefficient can be solved, which is then corrected for mass transfer effects, Eqs. (14) and (15). From known vapour phase concentrations, both in the bulk and at the interface, the condensing flux of each component can be

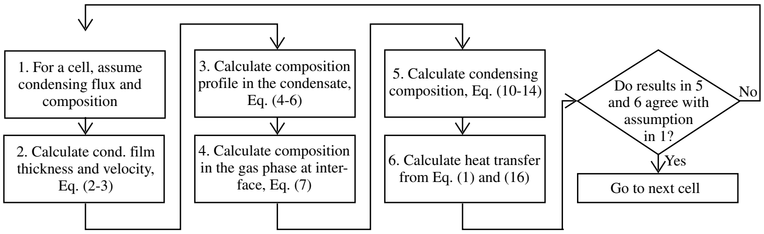

Fig. 2. Algorithm used for solving heat and mass transfer in a calculation cell.

calculated from Eqs. (10) and (11) together with the initial assumption of total flux. At the same time the heat balance is solved. First Eq. (1) expresses heat transferred from the vapour bulk to the interface, and then Eq. (18) expresses heat transferred from the interface through the condensate and tube wall into the cooling medium inside the tube. When the heat transfer, dQ, calculated in Eqs. (1) and (18) match, and when the flux of each component, calculated from Eqs. (10) and (11), agree with the assumptions, the correct solution of simultaneous heat and mass transfer is found for the present calculation cell, and calculations can move on to the next calculation cell.

3.2. Assumptions and simplifications

In order to carry out the calculations in an efficient way, a number of assumptions and simplifications are made. The geometry used in all calculations is a single column of ten horizontal, smooth tubes with an outside diameter, d_t, of 20 mm, where the smallest horizontal cross section area is varied. Condensation takes place on the outside of the tubes, with water flowing inside the tubes at a constant temperature of 293 K, and the condensate flow on the tubes is assumed to be laminar. No inter-phase heat or mass transfer is assumed to take place in the condensate flow between the tubes, nor is there any mixing within the condensate between the tubes. Liquid diffusion is considered in the direction normal to the tube, while it is neglected in the direction of the flow due to a relatively high liquid velocity. All thermophysical properties are calculated locally in each calculation cell from Refprop 7.0 [23].

A binary mixture of the refrigerants R134a and R32 with a composition of 50/50 by mole is used (corresponding to 66/34 by mass). The mixture has a temperature glide of around 5.5 K and both refrigerants are common in heat pump applications. Saturated vapour enters the top tube, and the pressure is adjusted to obtain total condensation and to make saturated liquid leave the bottom tube for two different average heat fluxes: $2000\,\mathrm{W\,m^{-2}\,s^{-1}}$ and $6000\,\mathrm{W\,m^{-2}\,s^{-1}}$. The higher heat flux is possibly higher than normal operation for a smooth tube, while the lower is a typical part load.

We start with one meter long tubes and a horizontal tube pitch of 1.25 times the tube diameter, d_t. The tube pitch is the horizontal distance between two tube centres positioned next to each other, imagining the column of tubes being mirrored. The tube pitch is varied from $1.1d_t$ up to $1.4d_t$ while the tube length is adjusted to maintain the total duty, resulting in a change in average heat flux. The change in tube pitch results in a change in vapour velocity, which in its turn influences the mass transfer resistance in the vapour phase. A smaller tube pitch will result in lower mass transfer resistance.

4. Results

4.1. Results without mass transfer resistance in the liquid

First, calculations without mass transfer resistance in the liquid phase are carried out as a reference. This is a common assumption when modelling condensation outside horizontal tubes. The lack of mass transfer resistance in the liquid results in a perfectly mixed condensate film, and it is simulated by giving the liquid diffusivity, D_{ij}, in Eq. (4) a high value. Results in terms of tube lengths required to maintain the average heat flux when the tube pitch is varied are given for the two heat fluxes in Fig. 3. The tube pitch factor on the x-axis multiplied by the tube diameter gives the total tube pitch. The influence of tube pitch on heat transfer area is only a little more than ±6% in the tube pitch interval for the lower heat flux, and less than ±2% for the high heat flux. A smaller tube pitch, i.e. a lower mass transfer resistance, results in shorter tubes, meaning better heat and mass transfer.

4.2. Results with mass transfer resistance in the liquid

Earlier results [13–15] have shown that the mixing of the liquid film probably is not perfect, but rather that it can be limited by diffusion. Therefore, calculations considering mass transfer resistance in the liquid phase are carried out. This is accomplished by using Eqs. (5) and (6) to estimate the binary liquid diffusivity used in Eq. (4). In Fig. 4, results in terms of tube lengths required to maintain total duty are presented. The results show the reverse of the trend shown in Fig. 3, implying better heat and mass transfer rates for a lower vapour velocity, i.e. when the tube pitch is larger. When increasing the tube pitch from $1.25d_t$ to $1.4d_t$ the area required is reduced more than 20% at the lower heat flux and around 8% at the higher heat flux. When decreasing the tube pitch from $1.25d_t$ to $1.1d_t$, the area required is increased by more than 50% at the lower heat flux and around

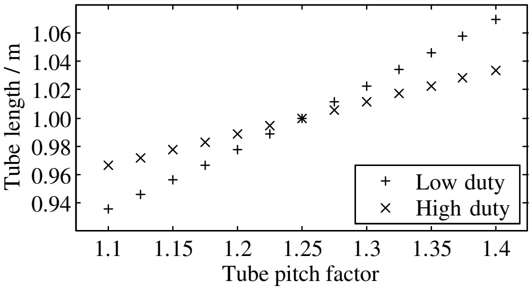

Fig. 3. Tube length required to maintain total duty as for tube pitch $1.25d_t$, when assuming no mass transfer resistance in the liquid. Tube pitch factor multiplied by the tube diameter gives the total tube pitch.

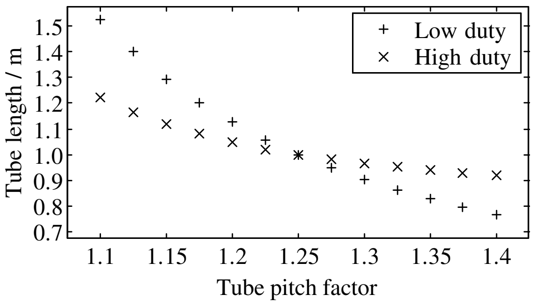

Fig. 4. Tube length required to maintain total duty as for tube pitch $1.25d_t$, when including mass transfer resistance in the liquid. Tube pitch factor multiplied by the tube diameter gives the total tube pitch.

20% at the higher heat flux, despite the lower mass transfer resistance. The question that arises is why the trend in Fig. 4 is the opposite of the trend presented in Fig. 3. This will be discussed in the following chapter.

5. Discussion

What is the reason for the unexpected behaviour that two mass transfer resistances in series result in better heat and mass transfer rates when the vapour phase resistance is higher? In the following discussion we try to give an explanation.

5.1. No mass transfer resistance in the liquid phase

The results without mass transfer resistance in the liquid phase are straightforward. A smaller tube pitch results in higher vapour velocity, and therefore higher heat and mass transfer coefficients, i.e. a lower mass transfer resistance, thus reducing the tube length required. It would, however, result in higher pressure drop if applied to a tube bundle in a condenser. The magnitude of the influence is relatively small.

5.2. Including mass transfer resistance in the liquid phase

In order to find an explanation for the somewhat surprising dependence on tube pitch when considering mass transfer resistance in the liquid phase, let us first check the behaviour of the mass transfer coefficient, $\beta^{\bullet}_{g,ij}$, in Eqs. (10) and (11). From this point we concentrate on the case with the higher heat transfer level only. Values of $\beta^{\bullet}_{g,ij}$ for this case are shown in Fig. 5 for three tube pitches: 1.1, 1.25 and 1.4 times the tube diameter d_t. The values plotted are averages for all calculation cells on each tube. The values of $\beta^{\bullet}_{g,ij}$ follow the values of h_g, according to Eq. (14), which are dependent on the vapour velocities. This can be seen in Fig. 5. The larger tube pitch results in lower mass transfer coefficients, corresponding to higher mass transfer resistance. The results in Fig. 5 do not explain the unexpected behaviour seen in Fig. 4.

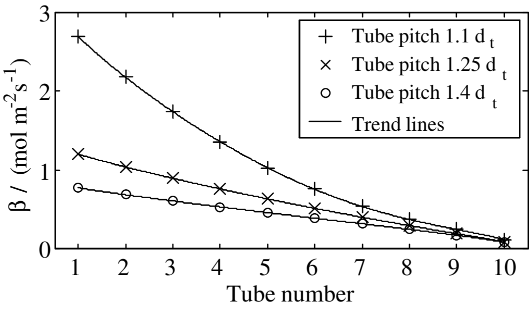

Fig. 5. Average tube values of mass transfer coefficient, $\beta_{g,ij}$, for three different tube pitches, $1.1d_t$ to $1.4d_t$.

Let us therefore proceed and check the behaviour of the composition of the condensing flux. In Fig. 6 the ratio of molar condensing flux R134a/R32 is plotted for two different tube pitches, $1.1d_t$ and $1.4d_t$, also here shown as tube averages. Of these two components R134a is the less volatile component, which can be seen in the figure by looking at the ratio for the first tube. With a small tube pitch, i.e. when the mass transfer resistance in the vapour is low, the ratio is over 1.5. This means a 50% higher condensation rate of R134a than of R32. The larger tube pitch, however, results in higher mass transfer resistance, and therefore the high rate of condensation for R134a cannot be maintained. The flux of R134a is hindered by the mass transfer resistance, resulting in a lower condensing flux ratio of approximately 1.25. The situation changes on the third tube, however. From the third tube and thereafter, the larger tube pitch results in a higher flux ratio. The reason for this is that more R134a remains in the bulk due to the higher resistance to mass transfer.

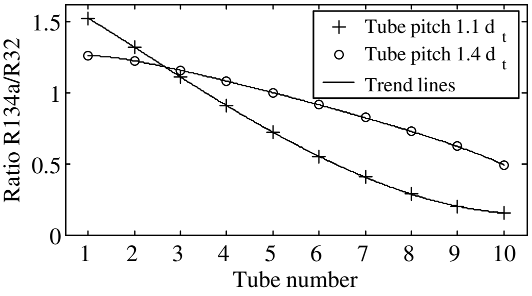

Fig. 6. Ratio of molar condensing flux R134a/R32 for two different tube pitches, $1.1d_t$ and $1.4d_t$, presented as averages over each tube.

Differences in flux ratios are connected to differences in compositions. In Fig. 7 bulk and interface compositions are plotted for the two tube pitches $1.1d_t$ and $1.4d_t$, again as tube averages. The higher condensation rate of R134a on the first tube for the smaller tube pitch results in higher concentration at the interface and lower concentration in the vapour bulk compared to the larger pitch, as illustrated by the dotted lines. During the course of condensation, the concentration of R134a is reduced both at the interface and in the bulk for both pitches, but due to the high condensation rate of R134a on the first tubes, the reduction will be more evident for the smaller tube pitch. Important in this matter is also the comparison of interface concentrations between the tube pitches. For a majority of the tubes, the smaller tube pitch results in a lower concentration of R134a at the interface. This means more of the more volatile component R32 at the interface, which will result in a lower interface temperature.

The interface temperatures for the two tube pitches can be seen in Fig. 8. From the third tube on, the smaller tube pitch results in a lower interface temperature than the larger tube pitch. The interface temperature is, for the conditions studied here, the most important factor for the heat transfer rate, since the heat is conducted from the interface with the interface temperature being the driving force. This becomes apparent when looking at the resulting average heat flux for each tube for the two tube pitches, shown in Fig. 9. The smaller tube pitch results in higher average heat flux on the first two tubes, but from the third tube on the larger tube pitch results in higher heat flux.

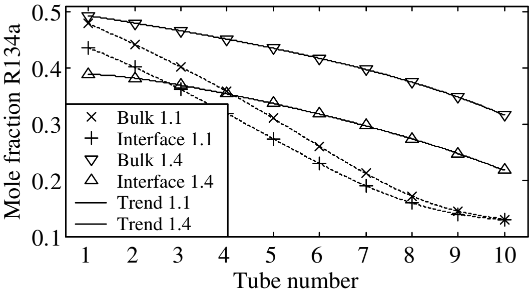

Fig. 7. Vapour mole fractions of R134a in the bulk and at the interface, presented at two different tube pitches, $1.1d_t$ and $1.4d_t$. The values presented are tube averages.

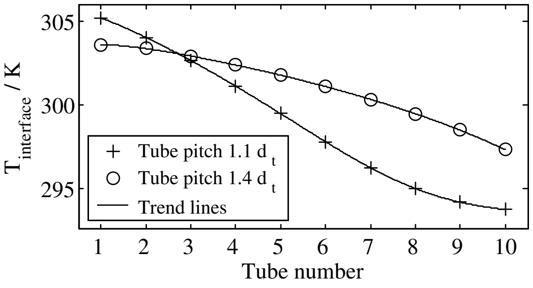

Fig. 8. Temperatures at the liquid interface for two tube pitches, $1.1d_t$ and $1.4d_t$. The values presented are tube averages.

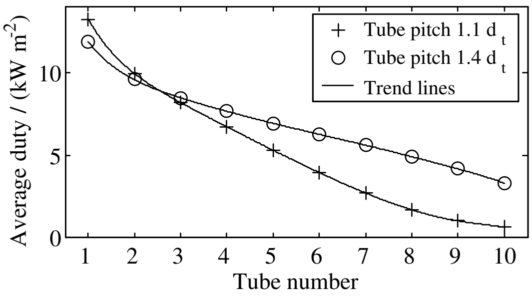

Fig. 9. Average heat flux presented tube-wise for two tube pitches, $1.1d_t$ and $1.4d_t$.

5.3. Summary of findings

The reasons for the unexpected behaviour seen in Fig. 4 for the combined effects of mass transfer resistances in both phases can now be accounted for. A larger tube pitch, and thus a higher mass transfer resistance, reduces the rate of heat and mass transfer on the first tubes. More importantly, it results in a lower relative condensation rate of the less volatile component, R134a in this case. A couple of tubes further down, there will still be a higher mass transfer resistance, but the fact that there is more remaining of the less volatile component in the vapour phase results in a higher fraction of the less volatile component in the newly formed condensate. This, and the fact that the condensate formed is not immediately transported into the condensate film due to the mass transfer resistance in the condensate, results in turn in higher interface temperature, and therefore also a larger temperature driving force. The larger driving force for heat transfer is a factor more significant than the higher mass transfer resistance in the vapour phase.

The results for the low level of heat flux are analogous to the results presented here for the high level of heat flux. They were only left out due to clarity and to lack of space. The magnitudes of the effects are however not quite as significant.

5.4. Further discussion

The three decisive assumptions, necessary in order to obtain the results presented here, are total condensation, velocity dependence on the mass transfer resistance in the vapour, and that the condensate flows in a laminar film over the tubes. The first two assumptions are straightforward, but the third can be questioned. A laminar film requires a smooth flow without disturbances with low enough Reynolds numbers not to be turbulent. At the high heat flux used in the calculations, the Reynolds number reaches 50. Fulford [24] reports in a review article a possible onset of waves at Reynolds numbers around 10, but also reports little influence on heat and mass transfer until Reynolds numbers reach 200–300. The reason is that a possible increased mixing only occurs at the surface, leaving a laminar sub-layer uninfluenced, implying that the assumption of diffusion as only mixing mechanism in the condensate is reasonable. How much a possible column or drop flow between two tubes influences the mixing is not investigated here, but several authors have investigated mass transfer in the flow between the tubes, for example Hu and Jacobi [25,26] and Yung et al. [27].

No experimental study has been carried out on the phenomenon presented in this paper yet. This theoretical study is aimed at enlightening the readers on the existence of the phenomenon, and to give an explanation of how it arises.

6. Conclusions

Detailed calculations have been carried out to investigate the combined effects of mass transfer resistances in the liquid phase and the vapour phase when condensing a binary zeotropic mixture on the outside of a horizontal tube bank. From the results and the discussion above the following conclusions can be drawn:

- A reduction of the mass transfer resistance in the vapour phase, e.g. by reducing the horizontal tube pitch, increases the area required for total condensation, quite contrary to the case where the condensate is perfectly mixed.
- The depletion of the less volatile component in the vapour bulk when there is a low mass transfer resistance in the vapour phase, increases the fraction of the light component condensing on the tubes further down. The insufficient mixing in the liquid causes the interface temperature to drop which reduces the heat transfer rate.

References

[1] A. Cavallini, G. Censi, D. Del Col, L. Doretti, G.A. Longo, L. Rosetto, C. Zilio, Condensation inside and outside smooth and enhanced tubes—a review of recent research, Int. J. Refrig. 26 (4) (2003) 373–392.
[2] Heat Exchanger Design Handbook, Hemisphere Publishing Corporation, New York, 1983.
[3] VDI Wärmeatlas, nineth ed., Springer-Verlag, Berlin, 2002.
[4] R.B. Bird, W.E. Stewart, E.N. Lightfoot, Transport Phenomena, second ed., John Wiley & Sons Inc., New York, 2002.
[5] J.G Collier, J.R. Thome, Convective Boiling and Condensation, third ed., Oxford University Press, 1994.
[6] K. Stephan, Heat Transfer in Condensation and Boiling, Springer-Verlag, Berlin, 1992.
[7] H. Honda, H. Takamatsu, N. Takata, Condensation of downward-flowing zeotropic mixture HCFC-123/HFC-134a on a staggered bundle of horizontal low-finned tubes, J. Heat Transfer 121 (2) (1999) 405–412.
[8] H. Honda, H. Takamatsu, N. Takata, Experimental measurement for condensation of downward-flowing R123/R134a in a staggered bundle of horizontal low-finned tubes with four fin geometries, Int. J. Refrig. 22 (8) (1999) 615–624.
[9] M. Belghazi, A. Bontemps, J.C. Signe, C. Marvillet, Condensation heat transfer of a pure fluid and binary mixture outside a bundle of smooth horizontal tubes. Comparison of experimental results and a classical model, Int. J. Refrig. 24 (8) (2001) 841–855.
[10] M. Belghazi, A. Bontemps, C. Marvillet, Experimental study and modeling of heat transfer during condensation of pure and binary mixture on a bundle of horizontal finned tubes, Int. J. Refrig. 26 (2) (2003) 214–223.
[11] D. Jung, C.B. Kim, S.M. Hwang, K.K. Kim, Condensation heat transfer coefficients of R22, R407C, and R410A on a horizontal plain, low fin, and turbo-C tubes, Int. J. Refrig. 26 (4) (2003) 485–491.
[12] D. Jung, K. Song, K. Kim, K. An, Condensation heat transfer coefficients of halogenated binary refrigerant mixtures on a smooth tube, Int. J. Refrig. 26 (7) (2003) 795–799.
[13] C. Gabrielii, L. Vamling, Replacement of R22 in shell-and-tube condensers: experiments and simulations, Int. J. Refrig. 20 (3) (1997) 165–178.
[14] D. Sajjan, T. Karlsson, L. Vamling, Reasons for drop in shell-and-tube condenser performance when replacing R22 with zeotropic mixtures—Part 1: Analysis of experimental findings, Int. J. Refrig. 27 (5) (2004) 552–560.
[15] T. Karlsson, L. Vamling, Reasons for drop in shell-and-tube condenser performance when replacing R22 with zeotropic mixtures—Part 2: Investigation of mass transfer resistance effects, Int. J. Refrig. 27 (5) (2004) 561–566.
[16] R. Taylor, R. Krishna, Multicomponent Mass Transfer, John Wiley & Sons Inc., New York, 1993.
[17] M.A. Siddiqi, K. Lucas, Correlations for prediction of diffusion in liquids, Can. J. Chem. Eng. 64 (1986) 839–843.
[18] E.N. Fuller, P.D. Schettler, J.C. Giddings, A new method for prediction of binary gas-phase diffusion coefficients, Ind. Eng. Chem. 58 (5) (1966) 19–27.
[19] T.H. Chilton, A.P. Colburn, Mass transfer (absorption) coefficients, prediction from data on heat transfer and fluid friction, Ind. Eng. Chem. 16 (11) (1934) 1183–1187.
[20] K.G. Schmidt, Wärmeübergang am quereangeströmten Rippenrohrbündel, in: VDI Wärmeatlas, eighth ed., Springer-Verlag, 1998.
[21] G. Ackermann, Forschungsheft 382 (1934) 1–16.
[22] A.P. Colburn, T.B. Drew, The condensation of mixed vapors, AIChE J. 33 (1937) 197–214.

[23] E.W. Lemmon, M.O. McLinden, M.L. Huber, NIST Standard Reference Database 23 (Refprop), version 7.0, Beta version, Physical and Chemical Properties Division, National Institute of Standards and Technology, 2002.

[24] G.D. Fulford, The flow of liquids in thin films, Adv. Chem. Eng. (5) (1964) 151–236.

[25] X. Hu, A.M. Jacobi, The intertube falling film, J. Heat Transfer (118) (1996) 616–625.

[26] X. Hu, A.M. Jacobi, Departure-site spacing for liquid droplets and jets falling between horizontal circular tubes, Exp. Therm. Fluid Sci. (16) (1998) 322–331.

[27] D. Yung, J.J. Lorenz, E.N. Ganic, Vapor/liquid interaction and entrainment in falling film evaporators, J. Heat Transfer (102) (1980) 20–25.